Gates, States, and Circuits:
Notes on the circuit model of quantum computation

Gavin E. Crooks

2020-06-03

Contents

1 Introduction

1.1 Additional reading

The canonical textbook for quantum computing and information remains Michael A. Nielsen's and Isaac L. Chuang's classic "Quantum Computation and Quantum Information" (affectionately know as Mike and Ike) [2, 3]. If you have any serious interest in quantum computing, you should own this book[1]. These notes are going to take a different cut through the subject, with more detail in some places, some newer material, but neglecting other areas entirely, since it is not nessary to repeat what Mike and Ike have already so ably covered. John Preskill's lecture notes [4] are also excellent (If perennially incomplete).

For a basic introduction to quantum mechanics, see "Quantum Mechanics: The Theoretical Minimum" by by Leonard Susskind and Art Friedman [5]. The traditional quantum mechanics textbooks are not so useful, since they tend to rapidly skip over the fundamental and informational aspects, and concentrate on the detailed behavior of light, and atoms, and cavities, and what have you. Such physical details matter if you're building a quantum computer, obviously, but not so much for programming, and I think the traditional approach tends to obscure the essentials of quantum information and how fundamentally different quantum is from classical physics. But among such physics texts, I'd recommend "Modern Quantum Mechanics" by J. J. Sakurai [6][2].

For gentler introductions to quantum computing see "Quantum Computing: A Gentle Introduction" by Eleanor G. Rieffel and Wolfgang H. Polak [7], and "Quantum Computing: An Applied Approach", by Jack D. Hidary [8]. Scott Aaronson's "Quantum Computing since Democritus" [9] is also a good place to start, particularly for computational complexity theory. Another interesting foray is "Quantum Country" by Andy Matuschak and Michael Nielsen, which is an online introductory course in quantum computing, with builtin spaced repetition [10].

Mathematically, quantum mechanics is applied linear algebra, and you can never go wrong learning more linear algebra. For a good introduction see "No Bullshit Guide to Linear Algebra" by Ivan Savov [11], and for a deeper dive "Linear Algebra Done Right" by Sheldon Axler [12].

For a deep dives into quantum information, both "The Theory of Quantum Information" by John Watrous [13] and "Quantum Information Theory" by Mark M. Wilde [14] are excellent, if weighty, tombs.

And if you have very young children, start them early with Chris Ferrie's "Quantum Computing for Babies" [15].

2 Single qubit gates

Classically, there are only 2 1-bit logic gates, identity and NOT. But in quantum mechanics the zero and one states can be placed into superposition, so there are many other possibilities.

2.1 Pauli gates

The simplest 1-qubit gates are the 4 gates represented by the Pauli operators: I, X, Y, and Z.

Pauli-I (identity):

$$\begin{pmatrix} 1 & 0 \\ 0 & 1 \end{pmatrix}$$

The trivial no-operation gate on 1-qubit, represented by the identity matrix.

Pauli-X gate (X-gate, NOT, bit flip)

$$\begin{pmatrix} 0 & 1 \\ 1 & 0 \end{pmatrix}$$

Applies a logical not to the computational basis, so that $|0\rangle$ becomes $|1\rangle$ and $|1\rangle$ becomes $|0\rangle$.

Pauli-Y gate (Y-gate) :

$$\begin{pmatrix} 0 & -i \\ i & 0 \end{pmatrix}$$

A useful mnemonic for remembering the matrix of the Y gate is "Minus eye high" [1].

Pauli-Z gate (Z-gate, phase flip)

$$\begin{pmatrix} 1 & 0 \\ 0 & -1 \end{pmatrix}$$

Phase gate

2.2 Rotation gates

R_x gate

$$R_x(\theta) = \begin{bmatrix} \cos(\frac{1}{2}\theta) & -i\sin(\frac{1}{2}\theta) \\ -i\sin(\frac{1}{2}\theta) & \cos(\frac{1}{2}\theta) \end{bmatrix} \tag{1}$$
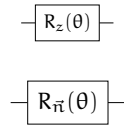
R_y gate

$$R_y(\theta) = \begin{bmatrix} \cos(\frac{1}{2}\theta) & -\sin(\frac{1}{2}\theta) \\ \sin(\frac{1}{2}\theta) & \cos(\frac{1}{2}\theta) \end{bmatrix} \tag{2}$$

R_z gate

$$R_z(\theta) = \begin{bmatrix} e^{-i\frac{1}{2}\theta} & 0 \\ 0 & e^{+i\frac{1}{2}\theta} \end{bmatrix} \qquad (3)$$

$$-\boxed{R_z(\theta)}-$$

$$-\boxed{R_{\vec{n}}(\theta)}-$$

$$R_{\vec{n}}(\theta) = \cos\frac{\theta}{2}I - i\sin\frac{\theta}{2}(n_xX + n_yY + n_zZ) \qquad (4)$$

$$R_{\vec{n}}(\theta) = \begin{bmatrix} \cos(\frac{1}{2}\theta) - in_z\sin(\frac{1}{2}\theta) & -n_y\sin(\frac{1}{2}\theta) - in_x\sin(\frac{1}{2}\theta) \\ n_y\sin(\frac{1}{2}\theta) - in_x\sin(\frac{1}{2}\theta) & \cos(\frac{1}{2}\theta) + in_z\sin(\frac{1}{2}\theta) \end{bmatrix}$$
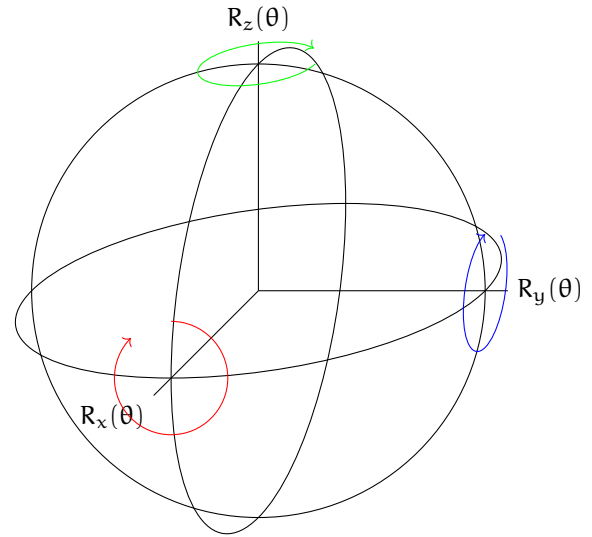$$(5)$$

2.3   Powers of Pauli gates

Phase shift   gate

S   (Phase, P, 'ess') gate

$$-\boxed{S}- \qquad \begin{pmatrix} 1 & 0 \\ 0 & i \end{pmatrix}$$

T   ("tee", $\pi/8$) gate

$$-\boxed{T}- \qquad \begin{pmatrix} 1 & 0 \\ 0 & e^{i\pi/4} \end{pmatrix}$$

2.4   Hadamard-type gates

Hadamard gate   The Hadamard gate is one of the most interesting and useful of the common gates. Its effect is a π rotation in the Bloch sphere about the axis $\frac{1}{\sqrt{2}}(\hat{x} + \hat{z})$, essentially half way between Z and X gates (fig. ???)

$$-\boxed{H}- \qquad \frac{1}{\sqrt{2}}\begin{bmatrix} 1 & 1 \\ 1 & -1 \end{bmatrix} \qquad \frac{1}{\sqrt{2}}\begin{bmatrix} 1 & 1 \\ 1 & -1 \end{bmatrix}$$

The Hadamard gate acts on the computation basis states to create superpositions of zero and one states.

$$H|0\rangle = \frac{1}{\sqrt{2}}(|0\rangle + |1\rangle) = |+\rangle$$
$$H|1\rangle = \frac{1}{\sqrt{2}}(|0\rangle - |1\rangle) = |-\rangle$$

Pseudo-Hadamard gate   [16]

$$-\boxed{h}- \qquad \frac{1}{\sqrt{2}}\begin{bmatrix} 1 & 1 \\ -1 & 1 \end{bmatrix}$$

$$-\boxed{h^\dagger}- \qquad \frac{1}{\sqrt{2}}\begin{bmatrix} 1 & -1 \\ 1 & 1 \end{bmatrix}$$
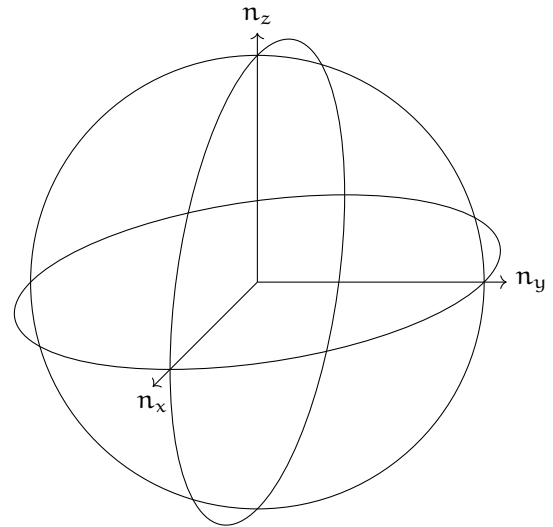

Figure 1: Rotations of the Bloch Sphere

Figure 2: Sphere of 1-qubit gates. Each point within this sphere represents a unique (up to phase) 1-qubit gate. Antipodal points on the surface represent the same gate.
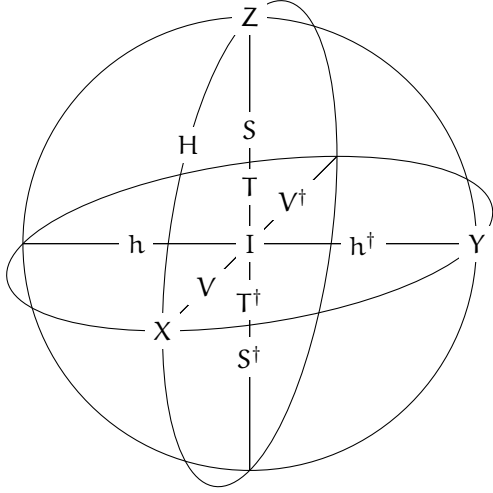
Figure 3: Coordinates of common 1-qubit gates

3 Decomposition of 1-qubit gates

3.1 ZYZ-Euler decompositions

3.2 General Euler decompositions

3.3 Bloch rotation decomposition

4 The canonical gate

The canonical gate is a 3-parameter quantum logic gate that acts on two qubits [1, 1, 1].

$$
\begin{aligned}
&\mathsf{CAN}(t_x, t_y, t_z) \\
&= \exp\!\left(-i\frac{\pi}{2}(t_x X \otimes X + t_y Y \otimes Y + t_z Z \otimes Z)\right)
\end{aligned} \tag{6}
$$

Here, $X = \left(\begin{smallmatrix} 0 & 1 \\ 1 & 0 \end{smallmatrix}\right)$, $Y = \left(\begin{smallmatrix} 0 & -i \\ i & 0 \end{smallmatrix}\right)$, and $Z = \left(\begin{smallmatrix} 1 & 0 \\ 0 & -1 \end{smallmatrix}\right)$ are the 1-qubit Pauli matrices.

Note that other parameterizations are common in the literature. Often there will be a sign flip and/or the $\frac{\pi}{2}$ factor is absorbed into the parameters. The parameterization used here the nice feature that it corresponds to powers of direct products of Pauli operators (up to phase) (see (12), (16), (??)) .
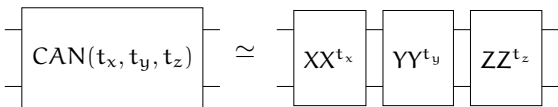
The canonical gate is, in a sense, the elementary 2-qubit gate, since any other 2-qubit gate can be decomposed into a canonical gate, and local 1-qubit interactions [17, 18, 19, 20].
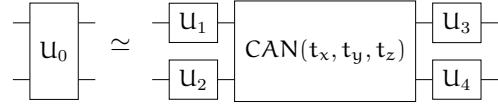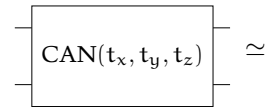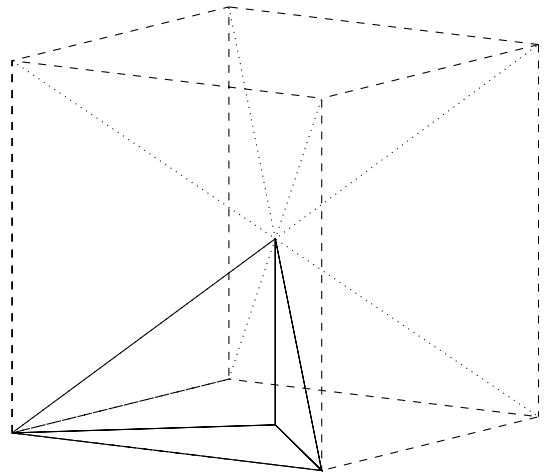

Here we use '≃' to indicate that two gates have the same unitary operator up to a global (and generally irrelevant) phase factor. We'll use '∼' to indicate that two gates are locally equivalent, in that they can be mapped to one another by local 1-qubit rotations.

The canonical gate is periodic in each parameters with period 4, or period 2 if we neglect a −1 global phase factor. Thus we can constrain each parameter to the range $[-1, 1)$. Since $X \otimes X$, $Y \otimes Y$, and $Z \otimes Z$ all commute, the parameter space has the topology of a 3-torus.

However, the canonical coordinates of any given 2-qubit gate are not unique since we have considerable freedom in the prepended and apended local gates. To remove these symmetries we can constrain the canonical parameters to a "Weyl chamber" [1, 1].

$$
(\tfrac{1}{2} \geqslant t_x \geqslant t_y \geqslant t_z \geqslant 0) \cup (\tfrac{1}{2} \geqslant (1-t_x) \geqslant t_y \geqslant t_z > 0) \tag{7}
$$

This Weyl chamber forms a trirectangular tetrahedron. All gates in the Weyl chamber are locally inequivalent (They cannot be obtained from each other via local 1-qubit gates). The net of the Weyl chamber is illustrated in Fig. 4, and the coordinates of many common 2-qubit gates are listed in table 1. Code for performing a canonical-decomposition, and therefore of determining the Weyl coordinates, can be found in the decompositions subpackage of QuantumFlow [21].

4

0 t_z $\frac{1}{2}$

Sycamore

QFT

SWAP

PSWAP $(\frac{1}{2}, \frac{1}{2}, t_z)$

iSWAP

Perfect entanglers

DB

DB

Perfect entanglers

$\sqrt{i\text{SWAP}}$

ECP

$\sqrt{\text{SWAP}}$ $\sqrt{\text{SWAP}}^\dagger$

$\sqrt{i\text{SWAP}}$

Weyl chamber of Canonical non-local 2-qubit gates

http://threeplusone.com/weyl

Gavin E. Crooks (2019)

Tech. Note 12v4

$$\text{CAN}(t_x, t_y, t_z) = \exp\left(-i\frac{\pi}{2}(t_x X \otimes X + t_y Y \otimes Y + t_z Z \otimes Z)\right)$$

CNOT

Exchange (t, t, t)

Exchange $(t, 1\text{-}t, 1\text{-}t)$

I   I

Ising $(t, 0, 0)$

0 t_x 0 $\frac{1}{2}$ 1

CV   CV

XY $(t, t, 0)$

XY $(t, 1\text{-}t, 0)$

Special orthogonal gates $(t_x, t_y, 0)$

Improper orthogonal gates $(\frac{1}{2}, t_y, t_z)$

t_y

B $\longrightarrow$

$\frac{1}{2}$

Instructions:
(1) Print
(2) Cut along outside edges
(3) Fold CPHASE, XY, EXCHANGE, and PSWAP edges
(4) Paste tabs

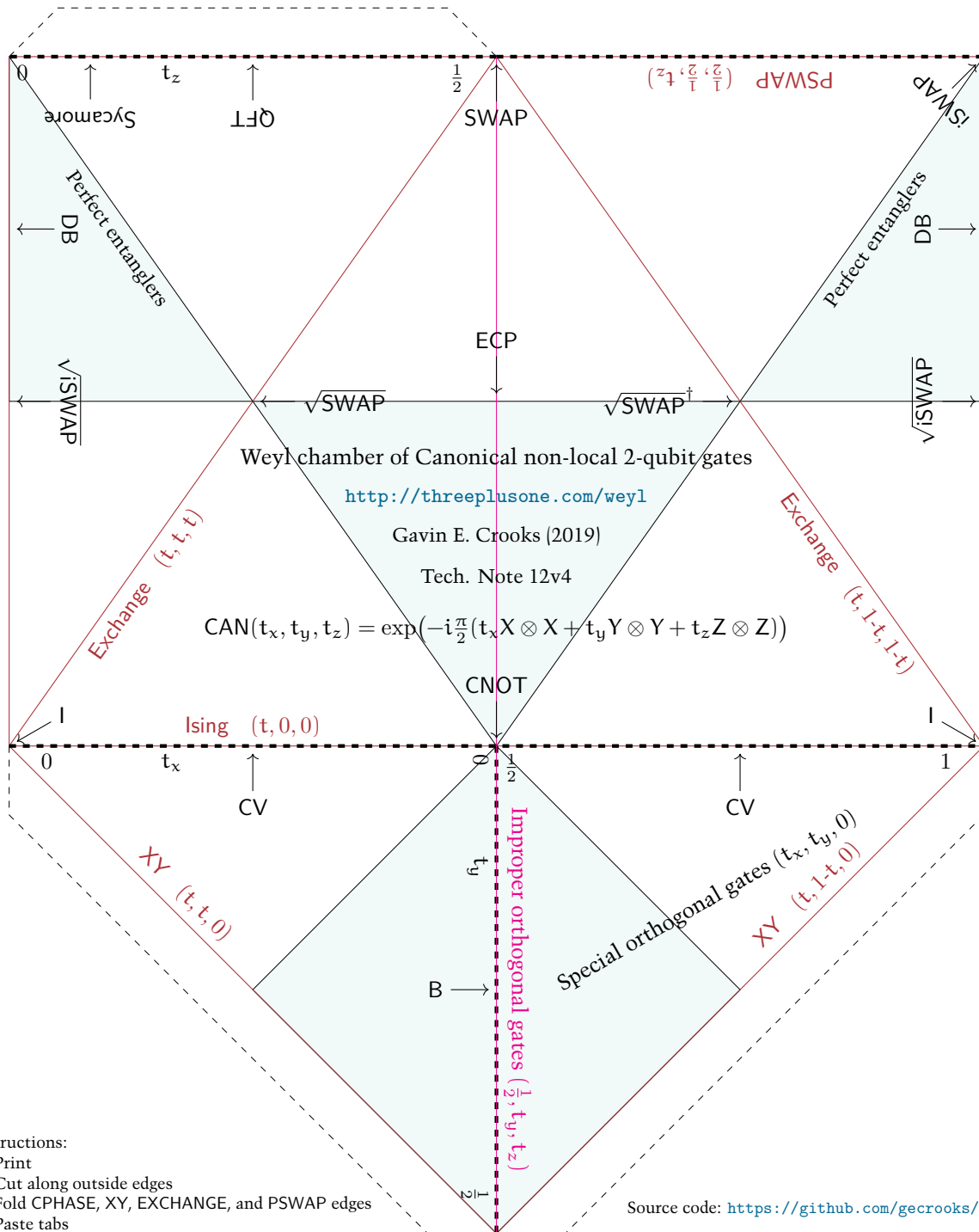Source code: https://github.com/gecrooks/weyl

Figure 4: The Weyl chamber of canonical non-local 2 qubit gates. (Print, cut, fold, and paste)
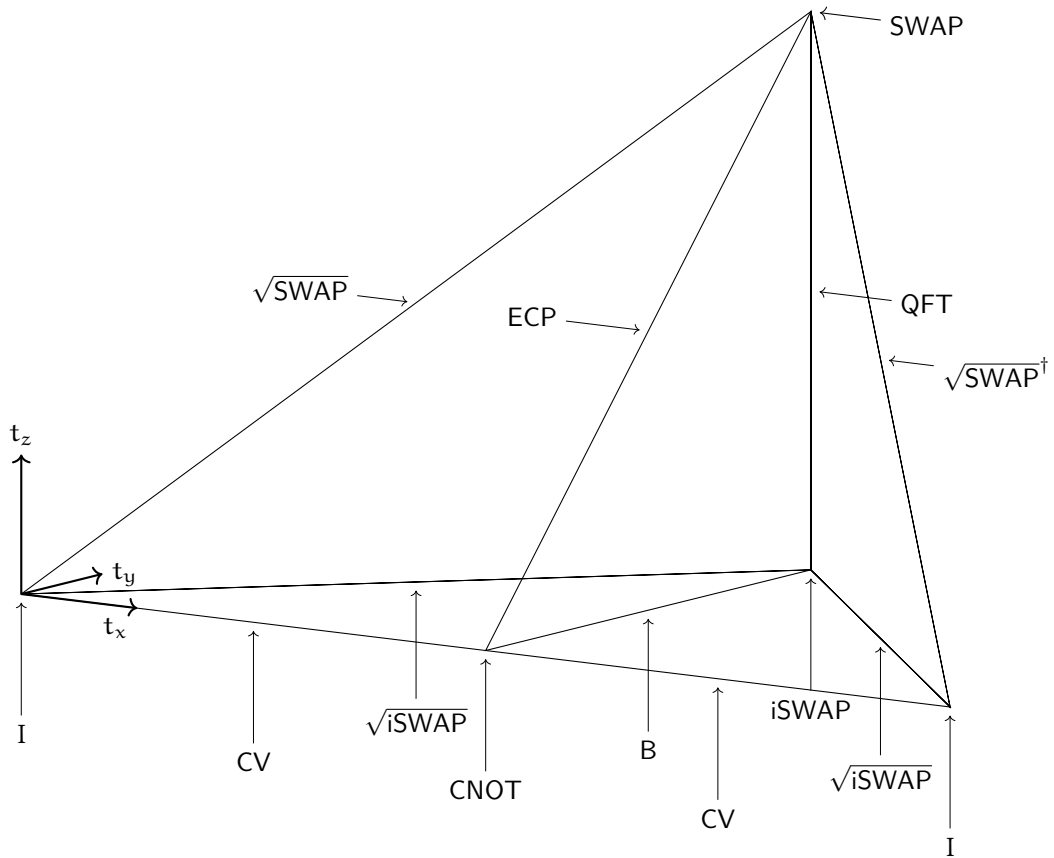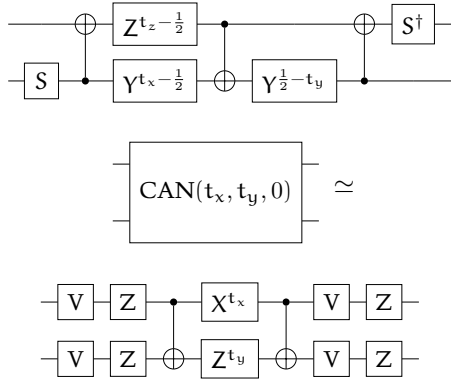
Figure 5: Location of the 11 principal 2-qubit gates in the Weyl chamber. All of these gates have coordinates of the form $\mathsf{CAN}(\frac{1}{4}k_x, \frac{1}{4}k_y, \frac{1}{4}k_z)$, for integer k_x, k_y, and k_z. Note there is a symmetry on the bottom face such that $\mathsf{CAN}(t_x, t_y, 0) \sim \mathsf{CAN}(\frac{1}{2} - t_x, t_y, 0)$.

5 Principal 2-qubit gates

5.1 Clifford gates

There are four unique 2-qubits gates in the Clifford group (up to local 1-qubit Cliffords): the identity, CNOT, iSWAP, and SWAP gates.

Identity gate

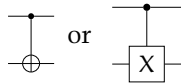$$I_2 = \begin{pmatrix} 1 & 0 & 0 & 0 \\ 0 & 1 & 0 & 0 \\ 0 & 0 & 1 & 0 \\ 0 & 0 & 0 & 1 \end{pmatrix} \tag{8}$$
$$= \mathsf{CAN}(0,0,0)$$

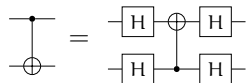**Controlled-NOT gate (CNOT, controlled-X, CX)**

$$\mathsf{CNOT} = \begin{pmatrix} 1 & 0 & 0 & 0 \\ 0 & 1 & 0 & 0 \\ 0 & 0 & 0 & 1 \\ 0 & 0 & 1 & 0 \end{pmatrix} \tag{9}$$
$$\sim \mathsf{CAN}(\tfrac{1}{2},0,0)$$

Commonly represented by the circuit diagrams

The CNOT gate is not symmetric between the two qubits. But we can switch control • and target ⊕ with local Hadamard gates.

iSWAP-gate

$$\mathsf{iSWAP} = \begin{pmatrix} 1 & 0 & 0 & 0 \\ 0 & 0 & i & 0 \\ 0 & i & 0 & 0 \\ 0 & 0 & 0 & 1 \end{pmatrix} \tag{10}$$
$$\simeq \mathsf{CAN}(-\tfrac{1}{2}, -\tfrac{1}{2}, 0)$$

Table 1: Canonical coordinates of common 2-qubit gates

Gate	t_x	t_y	t_z	t_x'	t_y'	t_z'
	$\leqslant\frac{1}{2}$			$>\frac{1}{2}$		
I_2	0	0	0	1	0	0
CNOT / CZ / MS	$\frac{1}{2}$	0	0			
iSWAP / DCNOT	$\frac{1}{2}$	$\frac{1}{2}$	0	$\frac{3}{4}$	$\frac{1}{2}$	0
SWAP	$\frac{1}{2}$	$\frac{1}{2}$	$\frac{1}{2}$			
CV	$\frac{1}{4}$	0	0	$\frac{3}{4}$	0	0
$\sqrt{\text{iSWAP}}$	$\frac{1}{4}$	$\frac{1}{4}$	0	$\frac{3}{4}$	$\frac{1}{4}$	0
DB	$\frac{3}{8}$	$\frac{3}{8}$	0	$\frac{5}{8}$	$\frac{3}{8}$	0
$\sqrt{\text{SWAP}}$	$\frac{1}{4}$	$\frac{1}{4}$	$\frac{1}{4}$			
$\sqrt{\text{SWAP}}^\dagger$				$\frac{3}{4}$	$\frac{1}{4}$	$\frac{1}{4}$
B	$\frac{1}{2}$	$\frac{1}{4}$	0			
ECP	$\frac{1}{2}$	$\frac{1}{4}$	$\frac{1}{4}$			
QFT_2	$\frac{1}{2}$	$\frac{1}{2}$	$\frac{1}{4}$			
Sycamore	$\frac{1}{2}$	$\frac{1}{2}$	$\frac{1}{12}$			
Ising / CPHASE	t	0	0			
XY	t	t	0	t	1-t	0
Exchange / SWAP$^\alpha$	t	t	t	t	1-t	1-t
PSWAP	$\frac{1}{2}$	$\frac{1}{2}$	t			
Special orthogonal	t_x	t_y	0			
Improper orthogonal	$\frac{1}{2}$	t_y	t_z			
XXY	t	t	δ	t	1-t	δ
	δ	t	t	δ	t	t

SWAP-gate

$$SWAP = \begin{pmatrix} 1&0&0&0 \\ 0&0&1&0 \\ 0&1&0&0 \\ 0&0&0&1 \end{pmatrix} \tag{11}$$

$$\simeq CAN(\tfrac{1}{2},\tfrac{1}{2},\tfrac{1}{2})$$
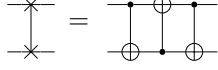
5.2 XX gates

Gates in the XX (or Ising) class have coordinates $CAN(t,0,0)$, which forms the front edge of the Weyl chamber. This includes the identity and CNOT gates.

XX gate (Ising)

$$XX(t) = e^{-i\frac{\pi}{2}tX\otimes X} \tag{12}$$

$$= \begin{pmatrix} \cos(\tfrac{\pi}{2}t) & 0 & 0 & -i\sin(\tfrac{\pi}{2}t) \\ 0 & \cos(\tfrac{\pi}{2}t) & -i\sin(\tfrac{\pi}{2}t) & 0 \\ 0 & -i\sin(\tfrac{\pi}{2}t) & \cos(\tfrac{\pi}{2}t) & 0 \\ -i\sin(\tfrac{\pi}{2}t) & 0 & 0 & \cos(\tfrac{\pi}{2}t) \end{pmatrix}$$

$$= CAN(t,0,0)$$

Mølmer-Sørensen gate (MS) [22, 23]

$$MS = \frac{1}{\sqrt{2}}\begin{pmatrix} 1&0&0&i \\ 0&1&i&0 \\ 0&i&1&0 \\ i&0&0&1 \end{pmatrix} \tag{13}$$

$$= CAN(-\tfrac{1}{2},0,0)$$

$$\sim CAN(\tfrac{1}{2},0,0)$$
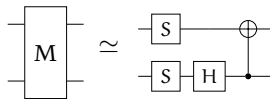
$$\sim CNOT$$

Proposed as a natural gate for laser driven trapped ions. Locally equivalent to CNOT. The Mølmer-Sørensen gate, or more exactly its complex conjugate $MS^{\dagger} = CAN(\tfrac{1}{2},0,0)$ is the natural canonical representation of the CNOT/CZ/MS gate family.

Magic gate (M) [1, 1, 1]

$$M = \frac{1}{\sqrt{2}}\begin{bmatrix} 1 & i & 0 & 0 \\ 0 & 0 & i & 1 \\ 0 & 0 & i & -1 \\ 1 & -i & 0 & 0 \end{bmatrix} \tag{14}$$

$$\sim CAN(\tfrac{1}{2},0,0) \tag{15}$$

[24]

YY gate

$$YY(t) = e^{-i\frac{\pi}{2}tY\otimes Y} \tag{16}$$

$$= \begin{pmatrix} \cos(\tfrac{\pi}{2}t) & 0 & 0 & +i\sin(\tfrac{\pi}{2}t) \\ 0 & \cos(\tfrac{\pi}{2}t) & -i\sin(\tfrac{\pi}{2}t) & 0 \\ 0 & -i\sin(\tfrac{\pi}{2}t) & \cos(\tfrac{\pi}{2}t) & 0 \\ +i\sin(\tfrac{\pi}{2}t) & 0 & 0 & \cos(\tfrac{\pi}{2}t) \end{pmatrix}$$

$$= CAN(0,t,0)$$

$$\sim CAN(t,0,0)$$

ZZ gate

$$ZZ(t) = e^{-i\frac{\pi}{2}tZ\otimes Z} \tag{17}$$

$$= \begin{pmatrix} 1 & 0 & 0 & 0 \\ 0 & e^{-i\pi t} & 0 & 0 \\ 0 & 0 & e^{-i\pi t} & 0 \\ 0 & 0 & 0 & 1 \end{pmatrix}$$

$$= CAN(0,0,t)$$

$$\sim CAN(t,0,0)$$

Controlled-Y gate

$$CY = \begin{pmatrix} 1&0&0&0 \\ 0&1&0&0 \\ 0&0&0&-i \\ 0&0&+i&0 \end{pmatrix} \tag{18}$$
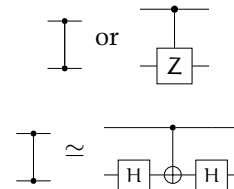
$$\sim CAN(\tfrac{1}{2},0,0)$$

Commonly represented by the circuit diagram:

Controlled-Z gate (CZ or CSIGN)

$$CZ = \begin{pmatrix} 1&0&0&0 \\ 0&1&0&0 \\ 0&0&1&0 \\ 0&0&0&-1 \end{pmatrix} \tag{19}$$
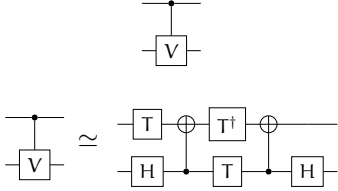
$$\sim CAN(\tfrac{1}{2},0,0)$$

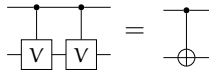Commonly represented by the circuit diagrams

8

Controlled-V gate (square root of CNOT gate):

$$CV = \begin{pmatrix} 1 & 0 & 0 & 0 \\ 0 & 1 & 0 & 0 \\ 0 & 0 & \frac{1+i}{2} & \frac{1-i}{2} \\ 0 & 0 & \frac{1-i}{2} & \frac{1+i}{2} \end{pmatrix} \tag{20}$$

$$\sim \mathsf{CAN}(\tfrac{1}{4}, 0, 0)$$

The CV gate is a square-root of CNOT, since the V-gate is the square root of the X-gate

Note that the inverse $CV^\dagger$ is a distinct square-root of CNOT. However CV and $CV^\dagger$ are locally equivalent, which is a consequence of the symmetry about $t_x = \frac{1}{2}$ on the bottom face of the Weyl chamber.

5.3 XY gates

Gates in the XY class forms two edges of the Weyl chamber with coordinates $\mathsf{CAN}(t, t, 0)$ (for $t \leqslant \frac{1}{2}$) and $\mathsf{CAN}(t, 1-t, 0)$ (for $t > \frac{1}{2}$). This includes the identity and iSWAP gates.

XY-gate Also occasionally referred to as the piSWAP (or parametric iSWAP) gate.

$$XY(t) = \begin{pmatrix} 1 & 0 & 0 & 0 \\ 0 & \cos(\pi t) & -i\sin(\pi t) & 0 \\ 0 & -i\sin(\pi t) & \cos(\pi t) & 0 \\ 0 & 0 & 0 & 1 \end{pmatrix} \tag{21}$$
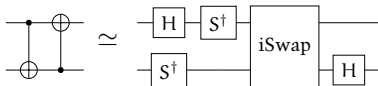
$$= \mathsf{CAN}(t, t, 0)$$

$$\sim \mathsf{CAN}(t, 1-t, 0)$$

Double Controlled NOT gate (DCNOT)

$$DCNOT = \begin{bmatrix} 1 & 0 & 0 & 0 \\ 0 & 0 & 0 & 1 \\ 0 & 1 & 0 & 0 \\ 0 & 0 & 1 & 0 \end{bmatrix} \tag{22}$$

$$\sim \mathsf{CAN}(\tfrac{1}{2}, \tfrac{1}{2}, 0)$$

Givens gate

$$\mathsf{Givens} = \exp(-i\theta(Y \otimes X - X \otimes Y)/2) \tag{23}$$

$$= \begin{bmatrix} 1 & 0 & 0 & 0 \\ 0 & \cos(\theta) & -\sin(\theta) & 0 \\ 0 & \sin(\theta) & \cos(\theta) & 0 \\ 0 & 0 & 0 & 1 \end{bmatrix} \tag{24}$$

$$\sim \mathsf{CAN}(\tfrac{1}{2}, \tfrac{1}{2}, 0)$$

bSWAP (Bell-Rabi) gate [25]

$$\mathsf{bSWAP} = \begin{pmatrix} 0 & 0 & 0 & -i \\ 0 & 1 & 0 & 0 \\ 0 & 0 & 1 & 0 \\ -i & 0 & 0 & 0 \end{pmatrix} \tag{25}$$
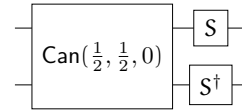
$$= \mathsf{CAN}(\tfrac{1}{2}, -\tfrac{1}{2}, 0)$$

$$\sim \mathsf{CAN}(\tfrac{1}{2}, \tfrac{1}{2}, 0)$$

???? gate

$$\begin{bmatrix} +1 & 0 & 0 & 0 \\ 0 & +1 & +1 & 0 \\ 0 & -1 & +1 & 0 \\ 0 & 0 & 0 & +1 \end{bmatrix} \tag{26}$$
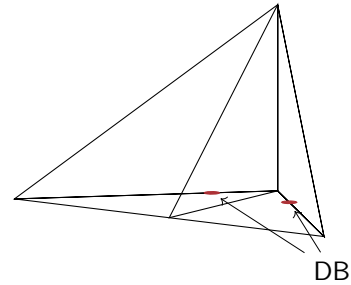
$$\sim \mathsf{Can}(\tfrac{1}{2}, \tfrac{1}{2}, 0)$$

Dagwood Bumstead (DB) gate [26] Of all the gates in the XY class, the Dagwood Bumstead-gate makes the biggest sandwiches. [26, Fig. 4]

$$DB = \begin{pmatrix} 1 & 0 & 0 & 0 \\ 0 & \cos(\frac{3\pi}{8}) & -i\sin(\frac{3\pi}{8}) & 0 \\ 0 & -\sin(\frac{3\pi}{8}) & \cos(\frac{3\pi}{8}) & 0 \\ 0 & 0 & 0 & 1 \end{pmatrix} \tag{27}$$

$$= XY(\tfrac{3}{8})$$

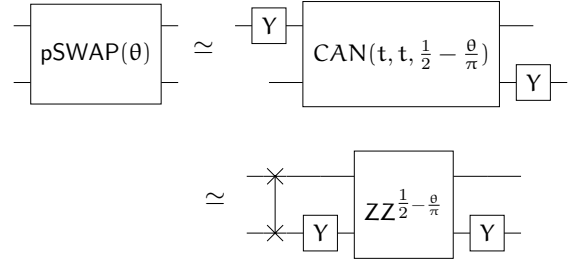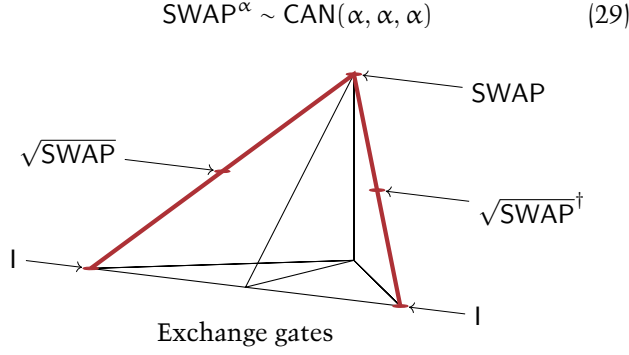$$= \mathsf{CAN}(\tfrac{3}{8}, \tfrac{3}{8}, 0)$$

5.4 Exchange-interaction gates

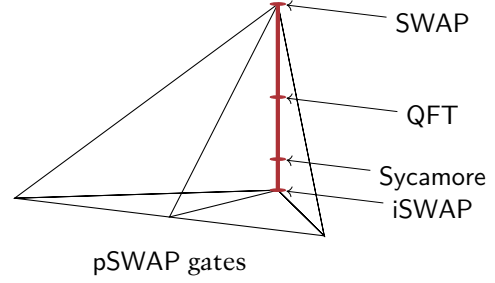Includes the identity and SWAP gates.

EXCH (XXX) gate

$$\mathsf{EXCH}(t) = \mathsf{CAN}(t, t, t) \tag{28}$$

SWAP-alpha gates

$$\mathsf{SWAP}^\alpha \sim \mathsf{CAN}(\alpha, \alpha, \alpha) \qquad (29)$$

Exchange gates

$\sqrt{\mathsf{SWAP}}$**-gate**

$$\sqrt{\mathsf{SWAP}} = \begin{pmatrix} 1 & 0 & 0 & 0 \\ 0 & \frac{1}{2}(1+i) & \frac{1}{2}(1-i) & 0 \\ 0 & \frac{1}{2}(1-i) & \frac{1}{2}(1+i) & 0 \\ 0 & 0 & 0 & 1 \end{pmatrix} \qquad (30)$$

$$= \mathsf{CAN}(\tfrac{1}{4}, \tfrac{1}{4}, \tfrac{1}{4})$$

Inverse $\sqrt{\mathsf{SWAP}}$**-gate**

$$\sqrt{\mathsf{SWAP}}^\dagger = \begin{pmatrix} 1 & 0 & 0 & 0 \\ 0 & \frac{1}{2}(1-i) & \frac{1}{2}(1+i) & 0 \\ 0 & \frac{1}{2}(1+i) & \frac{1}{2}(1-i) & 0 \\ 0 & 0 & 0 & 1 \end{pmatrix} \qquad (31)$$

$$= \mathsf{CAN}(\tfrac{3}{4}, \tfrac{1}{4}, \tfrac{1}{4})$$

Because of the symmetry around $t_x = \frac{1}{2}$ on the base of the Weyl chamber, the CNOT and iSWAP gates only have one square root. But the SWAP has two locally distinct square roots, which are inverses of each other.

5.5   Parametric SWAP gates

The class of parametric SWAP (PSWAP) gates forms the back edge of the Weyl chamber, $\mathsf{CAN}(\frac{1}{2}, \frac{1}{2}, t_z)$, connecting the SWAP and iSWAP gates. These gates can be decomposed into a SWAP and ZZ gate.
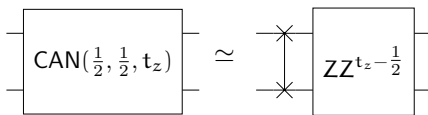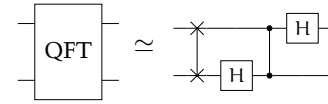

pSwap **gate**   (parametric swap) [27] The parametric swap gate as originally defined in the QUIL quantum programming language.

$$\mathsf{pSWAP}(\theta) = \begin{pmatrix} 1 & 0 & 0 & 0 \\ 0 & 0 & e^{i\theta} & 0 \\ 0 & e^{i\theta} & 0 & 0 \\ 0 & 0 & 0 & 1 \end{pmatrix} \qquad (32)$$

$$\sim \mathsf{CAN}(\tfrac{1}{2}, \tfrac{1}{2}, \tfrac{1}{2} - \tfrac{\theta}{\pi}) \qquad (33)$$

pSWAP gates

Quantum Fourier transform (QFT)   [1]

$$\mathsf{QFT} = \frac{1}{2} \begin{bmatrix} 1 & 1 & 1 & 1 \\ 1 & i & -1 & -i \\ 1 & -1 & 1 & -1 \\ 1 & -i & -1 & i \end{bmatrix} \qquad (34)$$

$$\sim \mathsf{CAN}(\tfrac{1}{2}, \tfrac{1}{2}, \tfrac{1}{4})$$

5.6   Orthogonal gates

An orthogonal gate, in this context, is a gate that can be represented by an orthogonal matrix (up to local 1-qubit rotations.) The special orthogonal gates have determinant $+1$ and coordinates $\mathsf{CAN}(t_x, t_y, 0)$, which covers the bottom surface of the canonical Weyl chamber.

Special orthogonal gates
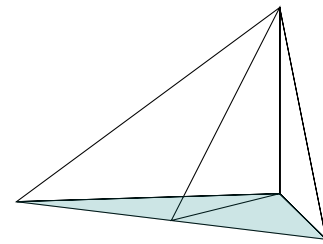
The improper orthogonal gates have determinant -1 and coordinates $\mathsf{CAN}(\frac{1}{2}, t_y, t_z)$, which is a plane connecting the CNOT, iSWAP, and SWAP gates.
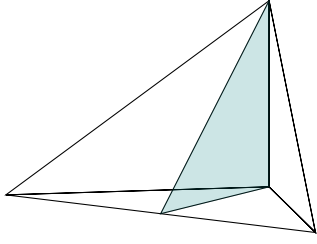
Improper orthogonal gates

B (Berkeley) gate [28] Located in the middle of the bottom face of the Weyl chamber.
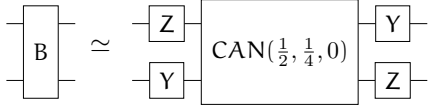
$$B = \begin{pmatrix} \cos(\frac{\pi}{8}) & 0 & 0 & i\sin(\frac{\pi}{8}) \\ 0 & \cos(\frac{3\pi}{8}) & i\sin(\frac{3\pi}{8}) & 0 \\ 0 & i\sin(\frac{3\pi}{8}) & \cos(\frac{3\pi}{8}) & 0 \\ i\sin(\frac{\pi}{8}) & 0 & 0 & \cos(\frac{\pi}{8}) \end{pmatrix}$$

$$= \frac{\sqrt{2-\sqrt{2}}}{2} \begin{pmatrix} 1+\sqrt{2} & 0 & 0 & i \\ 0 & 1 & i(1+\sqrt{2}) & 0 \\ 0 & i(1+\sqrt{2}) & 1 & 0 \\ i & 0 & 0 & 1+\sqrt{2} \end{pmatrix}$$

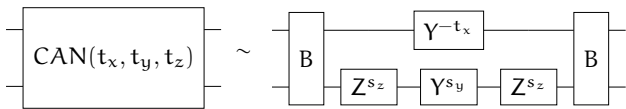$$= \mathsf{CAN}(-\tfrac{1}{2}, -\tfrac{1}{4}, 0)$$

(35)

The B-gate, as originally defined, has canonical parameters outside our Weyl chamber due to differing conventions for parameterization of the canonical gate. But of course it can be moved into our Weyl chamber with local gates.

The B-gate is half way between the CNOT and DCNOT (∼ iSWAP) gates, and thus it can be constructed from 3 CV (square root of CNOT) gates.
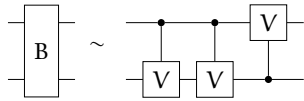
Notably two-B gates are sufficient to create any other 2-qubit gate (whereas, for example, we need 3 CNOT's in general) [28] [3]
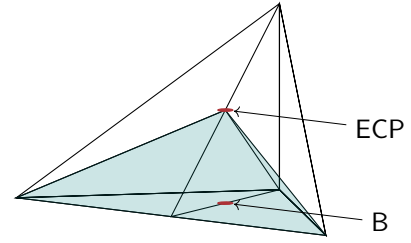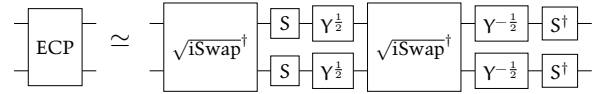

$$s_y = +\frac{1}{\pi}\arccos\left(1 - 4\sin^2\tfrac{1}{2}\pi t_y \cos^2\tfrac{1}{2}\pi t_z\right)$$

$$s_z = -\frac{1}{\pi}\arcsin\sqrt{\frac{\cos\pi t_y \cos\pi t_z}{1 - 2\sin^2\tfrac{1}{2}\pi t_y \cos^2\tfrac{1}{2}\pi t_z}}$$

(36)

ECP-gate [26]

$$\mathsf{ECP} = \frac{1}{2}\begin{pmatrix} 2c & 0 & 0 & -i2s \\ 0 & (1+i)(c-s) & (1-i)(c+s) & 0 \\ 0 & (1-i)(c+s) & (1+i)(c-s) & 0 \\ -i2s & 0 & 0 & 2c \end{pmatrix}$$

(37)

$$c = \cos(\tfrac{\pi}{8}) = \sqrt{\tfrac{2+\sqrt{2}}{2}}$$

$$s = \sin(\tfrac{\pi}{8}) = \sqrt{\tfrac{2-\sqrt{2}}{2}}$$

$$= \mathsf{CAN}(\tfrac{1}{2}, \tfrac{1}{4}, \tfrac{1}{4})$$

The peak of the pyramid of gates in the Weyl chamber that can be created with a square-root of iSWAP sandwich. Equivalent to $\mathsf{Can}(\tfrac{1}{2}, \tfrac{1}{4}, \tfrac{1}{4})$.

B and ECP gates, and ECP pyramid

W-gate [1]

$$W = \begin{bmatrix} 1 & 0 & 0 & 0 \\ 0 & \frac{1}{\sqrt{2}} & \frac{1}{\sqrt{2}} & 0 \\ 0 & \frac{1}{\sqrt{2}} & -\frac{1}{\sqrt{2}} & 0 \\ 0 & 0 & 0 & 1 \end{bmatrix}$$

$$\sim \mathsf{ECP} = \mathsf{CAN}(\tfrac{1}{2}, \tfrac{1}{4}, \tfrac{1}{4})$$

(38)

A 2-qubit orthogonal and Hermitian gate (and therefore also symmetric) $W^\dagger = W$, that applies a Hadamard gate to a duel-rail encoded qubit.
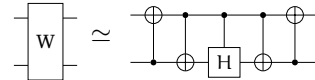
This W gate is locally equivalent to ECP,
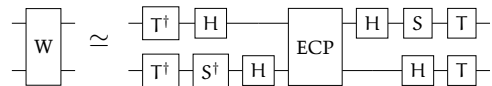
and thus three CNOT gates are necessary (and sufficient) to generate the gate.

$$\begin{array}{c}\framebox{W}\ \times\ \framebox{W}\end{array} = \begin{bmatrix} 1 & 0 & 0 & 0 \\ 0 & 1 & 0 & 0 \\ 0 & 0 & -1 & 0 \\ 0 & 0 & 0 & 1 \end{bmatrix}$$

5.7 XXY gates

The remaining faces of the Weyl chamber are the XXY family. Thanks to the Weyl symmetries, this family covers all three faces that meet at the SWAP gate.

$$\mathsf{XXY}(t,\delta) = \mathsf{CAN}(t,t,\delta) \tag{39}$$

FSIM (Ferminoic Simulator) gate [1]

Sycamore gate [1]

5.8 Perfect entanglers

Perfect entanglers

6 Multi-qubit gates

Toffoli gate (controlled-controlled-not, CCNOT)

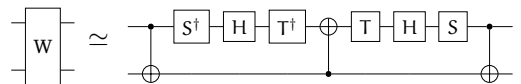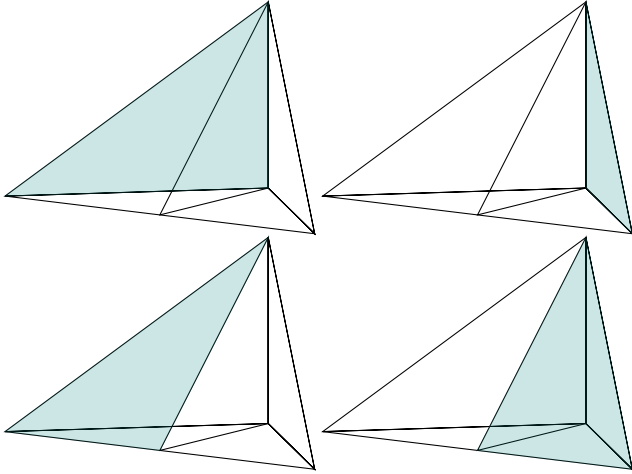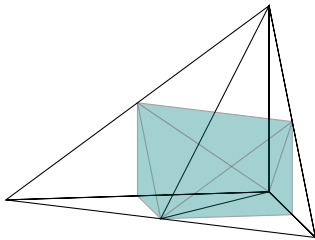$$\begin{bmatrix} 1 & 0 & 0 & 0 & 0 & 0 & 0 & 0 \\ 0 & 1 & 0 & 0 & 0 & 0 & 0 & 0 \\ 0 & 0 & 1 & 0 & 0 & 0 & 0 & 0 \\ 0 & 0 & 0 & 1 & 0 & 0 & 0 & 0 \\ 0 & 0 & 0 & 0 & 1 & 0 & 0 & 0 \\ 0 & 0 & 0 & 0 & 0 & 1 & 0 & 0 \\ 0 & 0 & 0 & 0 & 0 & 0 & 0 & 1 \\ 0 & 0 & 0 & 0 & 0 & 0 & 1 & 0 \end{bmatrix} \tag{40}$$

Fredkin gate (controlled-swap, CSWAP)

$$\mathrm{Fredkin} = \begin{bmatrix} 1 & 0 & 0 & 0 & 0 & 0 & 0 & 0 \\ 0 & 1 & 0 & 0 & 0 & 0 & 0 & 0 \\ 0 & 0 & 1 & 0 & 0 & 0 & 0 & 0 \\ 0 & 0 & 0 & 1 & 0 & 0 & 0 & 0 \\ 0 & 0 & 0 & 0 & 1 & 0 & 0 & 0 \\ 0 & 0 & 0 & 0 & 0 & 0 & 1 & 0 \\ 0 & 0 & 0 & 0 & 0 & 1 & 0 & 0 \\ 0 & 0 & 0 & 0 & 0 & 0 & 0 & 1 \end{bmatrix} \tag{41}$$

Peres gate [29]

$$\mathrm{Peres} = \begin{bmatrix} 1 & 0 & 0 & 0 & 0 & 0 & 0 & 0 \\ 0 & 1 & 0 & 0 & 0 & 0 & 0 & 0 \\ 0 & 0 & 1 & 0 & 0 & 0 & 0 & 0 \\ 0 & 0 & 0 & 1 & 0 & 0 & 0 & 0 \\ 0 & 0 & 0 & 0 & 0 & 0 & 0 & 1 \\ 0 & 0 & 0 & 0 & 0 & 0 & 1 & 0 \\ 0 & 0 & 0 & 0 & 0 & 1 & 0 & 0 \\ 0 & 0 & 0 & 0 & 1 & 0 & 0 & 0 \end{bmatrix} \tag{42}$$

Another gate that is universal for classical reversible computing. It is equivalent to a Fredkin followed by a CNOT gate.

CCZ gate (controlled-controlled-Z)

$$\begin{bmatrix} 1 & 0 & 0 & 0 & 0 & 0 & 0 & 0 \\ 0 & 1 & 0 & 0 & 0 & 0 & 0 & 0 \\ 0 & 0 & 1 & 0 & 0 & 0 & 0 & 0 \\ 0 & 0 & 0 & 1 & 0 & 0 & 0 & 0 \\ 0 & 0 & 0 & 0 & 1 & 0 & 0 & 0 \\ 0 & 0 & 0 & 0 & 0 & 1 & 0 & 0 \\ 0 & 0 & 0 & 0 & 0 & 0 & 1 & 0 \\ 0 & 0 & 0 & 0 & 0 & 0 & 0 & -1 \end{bmatrix} \tag{43}$$

Deutsch gate [30, 31, 32] A controlled-controlled-$iR_x(2\theta)$ gate. Mostly of historical interest, since this was the first quantum gate to be shown to be computationally universal [30]. Barenco [31] latter demonstrate a construction of the Deutsch gate from 2-qubit 'Barenco' gates, demonstrating that 2-qubits gates are sufficient for universality.

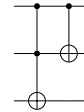$$\mathrm{Deutsch}(\theta) = \begin{bmatrix} 1 & 0 & 0 & 0 & 0 & 0 & 0 & 0 \\ 0 & 1 & 0 & 0 & 0 & 0 & 0 & 0 \\ 0 & 0 & 1 & 0 & 0 & 0 & 0 & 0 \\ 0 & 0 & 0 & 1 & 0 & 0 & 0 & 0 \\ 0 & 0 & 0 & 0 & 1 & 0 & 0 & 0 \\ 0 & 0 & 0 & 0 & 0 & 1 & 0 & 0 \\ 0 & 0 & 0 & 0 & 0 & 0 & i\cos(\theta) & \sin(\theta) \\ 0 & 0 & 0 & 0 & 0 & 0 & \sin(\theta) & i\cos(\theta) \end{bmatrix} \tag{44}$$
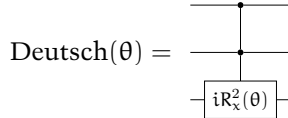
Examining the controlled unitary sub-matrix, the Deutsch gate can be thought of as a controlled $iR_X(\theta)^2$

gate.

$$\text{Deutsch}(\theta) = \quad \begin{array}{c} \bullet \\ \hline iR_x^2(\theta) \end{array}$$

7 Clifford Gates

The 1-qubit Clifford gates are those gates that can be generated by the phase (S), Hadamard (H), and controlled-not (CNOT) gates.

Notes

1. And Mike and Ike

2. At least partially because I had to slog through it, so why shouldn't you suffer too? It's a great book, but not easy.

3. Open Problem: Zang et al.[28] derive the analytic decomposition of the canonical gate to a B gate sandwich only up to local gates. Derive an analytic formula for the necessary local gates to complete the canonical to B-sandwich decomposition. (page 11)

References

[1] [citation needed]. (pages 2, 4, 4, 4, 4, 4, 8, 8, 8, 10, 11, 12, and 12).

[2] Michael A. Nielsen and Isaac L. Chuang. *Quantum Computation and Quantum Information*. Cambridge University Press (2000). (page 2).

[3] Michael A. Nielsen and Isaac L. Chuang. *Quantum Computation and Quantum Information: 10th Anniversary Edition*. Cambridge University Press (2000). (page 2).

[4] John Preskill. Quantum computation lecture notes (1997–2018). http://www.theory.caltech.edu/people/preskill/ph229/. (page 2).

[5] Leonard Susskind and Art Friedman. *Quantum Mechanics: The Theoretical Minimum*. Basic Books (2015). (page 2).

[6] J. J. Sakurai and Jim J. Napolitano. *Modern Quantum Mechanics*. Pearson, 2nd edition (2010). (page 2).

[7] Eleanor G. Rieffel. *Quantum Computing: A Gentle Introduction*. The MIT Press (2014). (page 2).

[8] Jack D. Hidary. *Quantum Computing: An Applied Approach*. Springer (2019). (page 2).

[9] Scott Aaronson. *Quantum Computing since Democritus*. Cambridge University Press (2013). (page 2).

[10] Andy Matuschak and Michael Nielsen. Quantum country (2019). https://quantum.country/. (page 2).

Table 2: Coordinates of the 24 1-qubit Clifford gates.

Gate	θ	n_x	n_y	n_z
I	0			
V	$\frac{1}{2}\pi$	1	0	0
X	π	1	0	0
V†	$-\frac{1}{2}\pi$	1	0	0
h†	$\frac{1}{2}\pi$	0	1	0
Y	π	0	1	0
h	$-\frac{1}{2}\pi$	0	1	0
S	$\frac{1}{2}\pi$	0	0	1
Z	π	0	0	1
S†	$-\frac{1}{2}\pi$	0	0	1
	π	$\frac{1}{\sqrt{2}}$	$\frac{1}{\sqrt{2}}$	0
H	π	$\frac{1}{\sqrt{2}}$	0	$\frac{1}{\sqrt{2}}$
	π	0	$\frac{1}{\sqrt{2}}$	$\frac{1}{\sqrt{2}}$
	π	$-\frac{1}{\sqrt{2}}$	$\frac{1}{\sqrt{2}}$	0
	π	$\frac{1}{\sqrt{2}}$	0	$-\frac{1}{\sqrt{2}}$
	π	0	$-\frac{1}{\sqrt{2}}$	$\frac{1}{\sqrt{2}}$
	$\frac{2}{3}\pi$	$\frac{1}{\sqrt{3}}$	$\frac{1}{\sqrt{3}}$	$\frac{1}{\sqrt{3}}$
	$-\frac{2}{3}\pi$	$\frac{1}{\sqrt{3}}$	$\frac{1}{\sqrt{3}}$	$\frac{1}{\sqrt{3}}$
	$\frac{2}{3}\pi$	$-\frac{1}{\sqrt{3}}$	$\frac{1}{\sqrt{3}}$	$\frac{1}{\sqrt{3}}$
	$-\frac{2}{3}\pi$	$-\frac{1}{\sqrt{3}}$	$\frac{1}{\sqrt{3}}$	$\frac{1}{\sqrt{3}}$
	$\frac{2}{3}\pi$	$\frac{1}{\sqrt{3}}$	$-\frac{1}{\sqrt{3}}$	$\frac{1}{\sqrt{3}}$
	$-\frac{2}{3}\pi$	$\frac{1}{\sqrt{3}}$	$-\frac{1}{\sqrt{3}}$	$\frac{1}{\sqrt{3}}$
	$\frac{2}{3}\pi$	$\frac{1}{\sqrt{3}}$	$\frac{1}{\sqrt{3}}$	$-\frac{1}{\sqrt{3}}$
	$-\frac{2}{3}\pi$	$\frac{1}{\sqrt{3}}$	$\frac{1}{\sqrt{3}}$	$-\frac{1}{\sqrt{3}}$

[11] Ivan Savov. *No bullshit guide to linear algebra.* Minireference Co. (2017). (page 2).

[12] Sheldon Axler. *Linear Algebra Done Right.* Springer, 2nd edition (2004). (page 2).

[13] John Watrous. *The theory of quantum information.* Cambridge University Press (2018). (page 2).

[14] Mark M. Wilde. *Quantum information theory.* Cambridge University Press, 2nd edition (2017). (page 2).

[15] Chris Ferrie and whurley. *Quantum Computing for Babie.* Sourcebooks Explore (2018). (page 2).

[16] J. A. Jones, R. H. Hansen, and M. Mosca. Quantum logic gates and nuclear magnetic resonance pulse sequences. *Journal of Magnetic Resonance*, 135(2):353–360 (1998). doi:10.1006/jmre.1998.1606. arXiv:quant-ph/9805070. (page 3).

[17] Jun Zhang, Jiri Vala, Shankar Sastry, and K. Birgitta Whaley. Geometric theory of nonlocal two-qubit operations. *Phys. Rev. A*, 67:042313 (2003). doi:10.1103/PhysRevA.67.042313. arXiv:quant-ph/0209120. (page 4).

[18] Jun Zhang, Jiri Vala, Shankar Sastry, and K. Birgitta Whaley. Optimal quantum circuit synthesis from controlled-unitary gates. *Phys. Rev. A*, 69:042309 (2004). doi:10.1103/PhysRevA.69.042309. ArXiv:quant-ph/0308167. (page 4).

[19] M. Blaauboer and R. L. de Visser. An analytical decomposition protocol for optimal implementation of two-qubit entangling gates. *J. Phys. A : Math. Theor*, 41:395307 (2008). doi:10.1088/1751-8113/41/39/395307. arXiv:cond-mat/0609750. (page 4).

[20] Paul Watts, Maurice O'Connor, and Jiří Vala. Metric structure of the space of two-qubit gates, perfect entanglers and quantum control. *Entropy*, 15:1963–1984 (2013). doi:10.3390/e15061963. (page 4).

[21] Gavin E. Crooks. QuantumFlow: A Quantum Algorithms Development Toolkit (2019). https://quantumflow.readthedocs.io/. (page 4).

[22] Klaus Mølmer and Anders Sørensen. Multiparticle entanglement of hot trapped ions. *Phys. Rev. Lett.*, 82:1835–1838 (1999). doi:10.1103/PhysRevLett.82.1835. (page 8).

[23] H. Häffner, C.F. Roos, and R. Blatt. Quantum computing with trapped ions. *Physics Reports*, 469(4):155–203 (2008). doi:10.1016/j.physrep.2008.09.003. (page 8).

[24] Farrokh Vatan and Colin Williams. Optimal quantum circuits for general two-qubit gates. *Phys. Rev. A*, 69:032315 (2004). doi:10.1103/PhysRevA.69.032315. ArXiv:quant-ph/0308006. (page 8).

[25] S. Poletto, Jay M. Gambetta, Seth T. Merkel, John A. Smolin, Jerry M. Chow, A. D. Córcoles, George A. Keefe, Mary B. Rothwell, J. R. Rozen, D. W. Abraham, Chad Rigetti, and M. Steffen. Entanglement of two superconducting qubits in a waveguide cavity via monochromatic two-photon excitation. *Phys. Rev. Lett.*, 109:240505 (2012). doi:10.1103/PhysRevLett.109.240505. (page 9).

[26] Eric C. Peterson, Gavin E. Crooks, and Robert S. Smith. Two-qubit circuit depth and the monodromy polytope. *Quantum*, 4:247 (2019). doi:10.22331/q-2020-03-26-247. arXiv:1904.10541. (pages 9, 9, and 11).

[27] Robert S. Smith, Michael J. Curtis, and William J. Zeng. A practical quantum instruction set architecture. ArXiv:1608.03355. (page 10).

[28] Jun Zhang, Jiri Vala, Shankar Sastry, and K. Birgitta Whaley. Minimum construction of two-qubit quantum operations. *Phys. Rev. Lett.*, 93:020502 (2004). doi:10.1103/PhysRevLett.93.020502. Quant-ph/0312193. (pages 11, 11, and 13).

[29] A. Peres. Reversible logic and quantum computers. *Phys. Rev. A*, 32(6):3266–3276 (1985). doi:10.1103/physreva.32.3266. (page 12).

[30] David Elieser Deutsch. Quantum computational networks. *Proc. R. Soc. Lond. A*, 425(1868):73–90 (1989). doi:10.1098/rspa.1989.0099. (page 12 and 12).

[31] Adriano Barenco. A universal two-bit gate for quantum computation. *Proceedings of the Royal Society of London. Series A: Mathematical and Physical Sciences*, 449(1937):679–683 (1995). doi:10.1098/rspa.1995.0066. (page 12 and 12).

[32] Xiao-Feng Shi. Deutsch, toffoli, and cnot gates via rydberg blockade of neutral atoms. *Phys. Rev. Applied*, 9:051001 (2018). doi:10.1103/PhysRevApplied.9.051001. (page 12).